NASA Technical Memorandum 88841

Estimation of High Temperature Low Cycle Fatigue on the Basis of Inelastic Strain and Strainrate

A. Berkovits
Lewis Research Center
Cleveland, Ohio

September 1986

NASA

ESTIMATION OF HIGH TEMPERATURE LOW CYCLE FATIGUE ON THE BASIS OF INELASTIC STRAIN AND STRAINRATE

A. Berkovits
National Aeronautics and Space Administration
Lewis Research Center
Cleveland, Ohio 44135

SUMMARY

Low-cycle fatigue life at high temperature can be predicted by introducing parametric values obtained from monotonic constitutive behavior into the Universal-Slopes Equation. For directionally solidified MAR-M200+Hf at 975 °C, these parameters are the maximum stress achievable under entirely plastic (time-independent) and purely creep (time-dependent) conditions and the corresponding inelastic strains, as well as the elastic modulus. For materials which exhibit plasticity/creep interaction, two more pairs of monotonic parameters must be evaluated for fatigue life prediction.

This life-prediction method based on the Universal-Slopes Equation, resulted from a constitutive model characterizing monotonic and cyclic data as inelastic strainrate as a function of inelastic strain. Characterizing monotonic data in this way, permitted distinction between different material responses such as strain-hardening, strain-softening, and dynamic recovery effects. Understanding and defining the region of influence of each of these effects facilitated formulation of the constitutive model in relation to the mechanical and microstructural processes occurring in the material under cyclic loading.

INTRODUCTION

Estimating fatigue life based on the strongly rate-dependent deformation processes which control material response at elevated temperature is a major problem in the design of turbomachinery (ref. 1). Such deformation processes include time-dependent creep and time-independent plasticity while strain is increasing in tension or compression during the fatigue cycle. Success in estimating low-cycle fatigue life under such conditions has varied considerably (refs. 2 to 5).

One of the more successful phenomenological methods for predicting high-temperature, low-cycle fatigue life is the strainrange partitioning approach, which was developed at NASA by Manson, Halford, and Hirschberg (ref. 6) and has become a viable engineering design tool (ref. 7). The procedure involves the determination of the four basic life relationships, resulting from the four possible combinations of plastic or creep strainrange in the tensile or

compressive halves of the fatigue cycle[1] for a given material, and their use in conjunction with an interaction damage rule to predict cyclic lives.

The present work was undertaken in order to achieve an understanding of the basic mechanisms which are responsible for observed material response, and thereby achieve a prediction model. Specific objectives were:

(1) Determination of the relationships between the mechanical response observed during strain-cycling tests and monotonic creep and plasticity materials response.

(2) Analysis of the plasticity and creep damage mechanisms operating during fatigue loading, through metallographic examination of the test specimens.

(3) Development of a model for the estimation of the strain-life relation, based on the mechanical and microstructural response.

In the present program (refs. 8 and 9) both cyclic and supporting monotonic tests were conducted under strain control at constant strainrates. The material tested was MAR-M200+2%Hf in directionally solidified form. Tests were conducted in air at 975 °C. The emphasis in this paper is on observed mechanical behavior. A more extensive discussion of microstructural response is found in reference 10.

MONOTONIC BEHAVIOR

Data for MAR-M200+2%Hf superalloy under constant strainrate in tension at 975 °C were used to construct the monotonic hodograph (fig. 1). The hodograph (refs. 11 and 12) is a convenient way of presenting materials response because the shapes of the constant-stress curves of the hodograph delineate the three mechanical processes governing materials response at elevated temperatures. It can be constructed from data obtained in a variety of mechanical tests, such as creep tests, relaxation tests, as well as strength tests. The hodograph is plotted as the logarithm of inelastic strainrate against the logarithm of inelastic strain in a family of constant-stress curves.

On the right-hand side of the hodograph the curves form a set of more or less parallel lines, with strainrate increasing for increasing strain. This region is governed by dynamic recovery of the material. It is bounded on the left by the minimum strainrate for a given stress, or conversely by the

---

[1]Throughout the discussion strainrange partitioning notation is used, namely:

Not.	Tensile loading	Compressive loading
PP	Plasticity	Plasticity
CC	Creep	Creep
PC	Plasticity	Creep
CP	Creep	Plasticity

maximum stress developed under a given strainrate. On the right the region is bounded by the fracture strain, which is constant at the lower strainrates which characterize creep, and decreases somewhat in the high-strainrate, plasticity-affected regime.

Plasticity is the dominant process in the upper left-hand quadrant of the hodograph. Here the vertical lines indicate a stress-strain relationship that is independent of the strainrate. At these relatively high strainrates, dislocation locking akin to strain-aging does not begin to be felt until considerable strain has taken place under strain-hardening conditions. In fact, by the time strain-aging-like effects can take place in this range they are over-shadowed by the recovery process which eventually leads to failure. The lower bound of the plasticity region is defined by a time-constant controlled by the material diffusion rates. This recovery boundary is indicated in the figure by the 45° line.

Dislocation generation, pile-ups and interactions, causing a hardening effect, dominate the lower left quadrant of the hodograph. At low strainrates, low to moderate stresses develop due to dislocation climb and diffusion processes in the material. Recovery rates at the low energy levels involved here are overshadowed until substantial strain is achieved. The diffusion processes are increasingly inhibited by continuing locking, with the result that strainrate decreases as constant stress is maintained, until sufficient strain is accumulated so that recovery becomes the dominant cause of straining.

Thus the monotonic hodograph defines an area where time-independent strain occurs at high-strainrates prior to initiation of the recovery process, and a region of time-independent deformation at more moderate strainrates. Time-dependent deformation is caused by dynamic recovery in the material, evidenced as straining initiated at moderate strainrate and again when failure is approached. Between these extremes dislocation locking mechanisms retard deformation and lead to transitory hardening of the material. These characteristics of monotonic straining have been emphasized because of their significance regarding cyclic response.

CYCLIC BEHAVIOR

Results of cyclic strain-controlled tests are shown in the cyclic hodograph of figure 2. The tests were conducted under symmetrical loading ($R_\varepsilon = -1.0$), so that in reality two hodographs, one for tension and one for compression, are required. However, as was the case under monotonic loading (ref. 9), tensile and compressive responses were found to coincide, and it was possible to present both on the same plot by using absolute values of the parameters.

In order to superimpose cyclic stresses and strains on the monotonic hodograph, as in figure 2, adjustment must be made for the fact that cyclic loading has double the range of the corresponding monotonic excursion. Thus the points on the hysteresis loop were plotted as $\Delta\sigma/2$ and $\Delta\varepsilon_{in}/2$, with the compressive load-reversal point as reference. In this way the cyclic strain-strainrate-stress values became compatible with monotonic curves, and could easily be compared with them.

The cyclic response curves obtained were unique functions of total strainrate which was held constant throughout each cyclic test. For a given total strainrate or frequency a single straight line resulted, regardless of strain amplitude, above the recovery demarcation line for PP tests and below it for CC tests. The plasticity half of CP and PC hysteresis loops coincided with PP results, while the creep half matched results obtained from CC tests.

PP results in figure 2 indicate that for a given plastic strainrate, doubling the loading frequency resulted in essentially doubling the corresponding plastic strain. This is due to the fact that at plastic strain amplitude on the order of 0.5 percent and less, the plastic stress-strain response was almost linear. The relationship between cyclic PP results and monotonic plasticity is not immediately evident. However, as will be brought out in the discussion of CC data and their bearing on fatigue life prediction, the relation of the cyclic/monotonic parameters is secondary.

If the CC results are cross plotted as lines of constant stress in the manner of the monotonic hodograph, the curves of figure 3 are obtained. At frequencies below 0.01 Hz cyclic data coincided with monotonic data, probably because at such low frequencies the loading is essentially static. However, at frequencies between 0.01 and 0.04 Hz, constant stress curves remained essentially horizontal at the level determined by the intersection of the monotonic hodograph and the straight line representing the initiation of time-dependent recovery processes. In this frequency range hardening did not occur under cyclic loading, the material remaining almost fully recovered and soft. This suggests that radically different characteristics were active in the microstructure under cyclic and monotonic conditions, before the onset of the cracking and failure phase. Similar response under cyclic conditions was noticed previously (refs. 13 and 14) for Udimet-700 and for 316 stainless steel.

The phenomenon of preserved "softness" of the material under cyclic conditions has also been noted by others (ref. 15). It is apparently the result of relaxation of dislocation back stress and pile up during reverse loading, so that the material responds as if it were virgin material following each load reversal. In this respect the cyclic response is quite different from monotonic behavior. Note in particular that all the cyclic hodograph lines in the creep region seem to converge at a single point. This will be of significance when fatigue life prediction is discussed in the next section.

STRAINRANGE PARTITIONED LIFE PREDICTION

The crux of the study of constitutive behavior of materials is its use in predicting failure. This objective has seldom been achieved (ref. 16). Fatigue-life data obtained from MAR-M200+Hf material at 975 °C will now be presented and discussed. A method of predicting fatigue life, based on the monotonic hodograph, will be proposed. Results of strainrange partitioned tests conducted under constant strainrates are shown as strain-life curves in figure 4. The PP-life curve shows significantly longer lives than CC, PC or CP results. The latter all have similar fatigue lives, because there are almost no transverse grain boundary segments to act as crack initiation sites under tensile creep conditions in the directionally solidified material (ref. 17). In all cases detectable fatigue cracks developed only during the last

20 percent of the cyclic tests. Somewhat more oxidation occurred on the crack face in tests during which the tensile phase was at low strainrate (CC and CP) than in those with high tensile strainrate (PP and PC).

Prediction of fatigue life for loading frequencies which engender creep phenomena requires more than constitutive information alone. Although at some frequencies both strain and stress depend only on strainrate and are essentially independent of each other, at yet lower frequencies the monotonic strain-strainrate-stress relation appears to hold for cyclic loading as well, as shown in figure 3. On the other hand the data of figure 4 indicate that strain-life is independent of frequency and strainrate. The key to cyclic-creep life prediction is to be found by interpretation of the cyclic and monotonic hodographs in terms of the controlling deformation process. It was shown previously that the monotonic hodograph clearly defines recovery-controlled deformation by the positive sloping curves in the high-strain region, and the similar line which separates the plasticity and dynamic recovery regimes. These curves can be modeled as a family of straight and parallel lines, as in figure 5, and can be related to the diffusion energy relation. The hardening process which occurs at low strains can be described as a family of parabolas emanating from the recovery initiation line and intersecting the recovery family at some intermediate strain. The line of intersection of the two families of curves which represent the controlling processes, is significant when attention is turned to the cyclic loading case.

All the cyclic creep curves of the hodograph (fig. 3) appear to converge at a unique point. Stress amplitudes above 300 MPa indicate some cyclic hardening, while lower stress amplitudes exhibit cyclic softening in approaching this point. Very low frequency tests undergo hardening similar to monotonic tests at commensurate strainrates; as for higher frequencies, these cyclic results also converge to the same point. The fact that this point falls on the line of maximum stresses for given strainrates, and on the recovery curve for a stress of 600 MPa, may not be coincidental. Failure due to the dynamic recovery processes occurs in the creep region at an upper stress limit of approximately 600 MPa. The recovery mechanism appears to be coarsening of the γ' precipitate particles (ref. 10). At higher stresses failure is still due to recovery, although it comes after plastic deformation. Here the recovery mechanisms is dissolution of the γ', and ductility is reduced as a result of the earlier plastic deformation. (An extensive discussion of microstructural developments is given in ref. 10.)

Thus the stress and strain coordinates, 600 MPa and 0.007 respectively, are sufficient to define conditions leading to failure under the completely relaxed creep cycling, which control CC, CP and PC failure in the MAR-M200+Hf material under discussion. On this basis a relation of the Universal-Slopes type can be suggested as

$$\frac{\Delta\varepsilon}{2} = \frac{\sigma_{UCC}}{E} N^{-0.12} + \varepsilon_{UCC}^{0.6} N^{-0.6} \qquad (1)$$

where σ_{UCC} is the ultimate time-dependent stress (equal to 600 MPa in MAR-M200+Hf at 975 °C), and ε_{UCC} is the corresponding time-dependent strain (equal to 0.007 in MAR-M200+Hf at 975 °C). The strain-life curve calculated from the above equation is shown in figure 4. Correlation of calculated results with experimental CC, CP, and PC data is excellent.

The present contention, that fatigue life is determined by the material response at its maximum monotonic strength, before the onset of dynamic recovery leading to failure, was applied to PP data as well. Maximum stress under plasticity conditions occurred in the material investigated at σ_{UPP} equal to 900 MPa. The corresponding plastic strain ε_{UPP} was approximately 0.007, the same value as for ε_{UCC}. These values of the constitutive parameters were substituted in a PP relation of the form:

$$\frac{\Delta\varepsilon}{2} = \frac{\sigma_{UPP}}{E} N^{-0.12} + \varepsilon_{UPP}^{0.6} N^{-0.6} \qquad (2)$$

Calculated results, shown as a line in the life curve of figure 4, again indicate very good agreement with experimental PP data.

LIFE PREDICTION FOR OTHER MATERIALS

In directionally solidified MAR-M200+Hf material CP and PC fatigue life was dominated by the creep loading. More importantly the plasticity half of the strain cycle did not significantly affect the response of the creep half of the hysteresis loop. As a result, the creep parameters remained the controlling factors in CP and PC life. However, in other materials the effect of compressive plasticity on the subsequent tensile creep half-cycle, in a CP test, and that of compressive creep on subsequent tensile plasticity in a PC test must be quantified in order to predict CP and PC lifetimes from the Universal Slopes Equation. The appropriate values of σ_U and ε_U may be determined from the tensile side of one-cycle-to-failure tests, in which compressive stress and strain equivalent to the negative of the maximum (P or C) stress and strain are applied prior to tensile (C or P respectively) loading to failure. The validity of this approach is now being investigated for a number of other elevated temperature materials.

The principle of applying the maximum achievable stress (true ultimate tensile strength) and the corresponding inelastic strain is comparable with Universal-Slopes parameters at temperatures not involving time-dependent phenomena. At room temperature, for example, maximum true stress occurs at or near specimen failure, and the corresponding inelastic strain is essentially the true ductility of the material. At elevated temperature the maximum stress occurs earlier in the monotonic test, since considerable straining under dynamic recovery control occurs after the strength of the material has been exhausted.

CONCLUSION

Presentation of monotonic and cyclic data as inelastic strainrate against inelastic strain differentiates between strain-hardening, softening and dynamic recovery. Defining and quantifying these effects facilitate formulation of a mode based on mechanical and microstructural processes. Thus a potentially useful tool for predicting high-temperature creep-fatigue life from monotonic properties was developed.

REFERENCES

1. Turbine Engine Hot Section Technology 1983. NASA CP-2289, 1983.

2. Fong, J.T., ed.: Fatigue Mechanisms. ASTM-STP-675, ASTM, 1979.

3. Burke, J.J.; and Weiss, V., eds.: Fatigue Environment and Temperature Effects. Plenum 1983.

4. Amzallag, C.; Leis, B.N.; and Rabbe, P., eds.: Low-Cycle Fatigue and Life Prediction. ASTM-STP-770, ASTM, 1982.

5. Brunetaud, R., et al., eds.: High Temperature Alloys for Gas Turbines 1982. D. Reidel, 1982.

6. Manson, S.S.; Halford, G.R.; and Hirschberg, M.H.: Creep-Fatigue Analysis by Strain-Range Partitioning. Symposium on Design for Elevated Temperature Environment, S.Y. Zamrik, ed., ASME, 1971, pp. 12-28.

7. Deutsch, G.C., ed.: Characterization of Low Cycle High Temperature Fatigue by Strainrange Partitioning Method. AGARD-CP-243, AGARD, France, 1978.

8. Berkovits, A.; and Nadiv, S.: Constitutive Relationships for Creep-Fatigue in High-Temperature Materials. Mechanical Behavior of Materials-IV, Vol. 1, J. Carlsson and N.G. Ohlson, eds., Pergamon, 1984, pp. 149-156.

9. Berkovits, A.; and Nadiv, S.: Creep-Fatigue in PWA 1422 Material. Proceedings of the V International Congress on Experimental Mechanics, Society for Experimental Stress Analysis, 1984, pp. 664-669.

10. Nadiv, S.; Berkovits, A.; and Shalev, G.: Paper presented at the International Conference on Fatigue, Corrosion Cracking, Fracture Mechanics, and Failure Analysis, Salt Lake City, UT, Dec. 3-6, 1985, to be published, ASM, Metals Park, OH, 1986.

11. Berkovits, A.: Hodographic Approach to Predicting Inelastic Strain at High Temperature. NASA TN D-6937, 1972.

12. Berkovits, A.: Prediction of Inelastic High Temperature Materials Behavior by Strain-Rate Approach. J. Eng. Mater. Technol., Vol. 96, No. 2, Apr. 1974, pp. 104-108.

13. Berkovits, A.: Hodographic Prediction of Cyclic Creep Behavior. J. Aircr. Vol. 11, No. 1, Jan. 1974, pp. 10-14.

14. Berkovits. A.: Unpublished Data.

15. Kear, B.H.; and Oblak, J.M.: Deformation Modes in Gamma-Prime Precipitation-Hardened Nickel-Base Alloys [MAR-M200]. J. Phys. (Paris), Vol. 35, Dec. 1974, Suppl., pp. C7-35 to C7-45.

16. Nonlinear Constitutive Relations for High Temperature Applications. NASA CP-2271, 1983.

17. Manson, S.S.; and Halford, G.R.: Complexities of High Temperature Metal Fatigue: Some Steps Toward Understanding. Israel J. Technology, Vol. 21, No. 1-2, 1983, pp. 29-54.

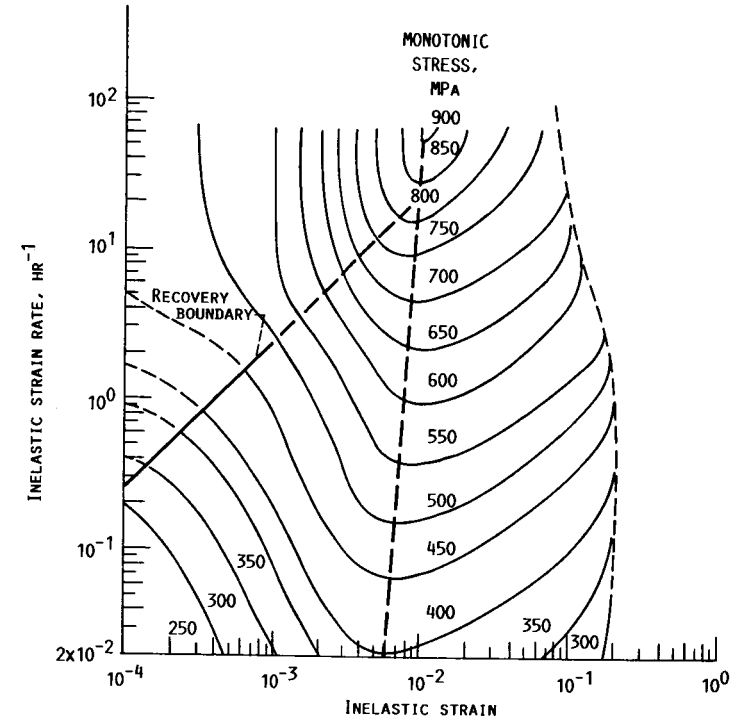

FIGURE 1.- MONOTONIC HODOGRAPH OF MAR-M200+HF AT 975 ^{o}C.

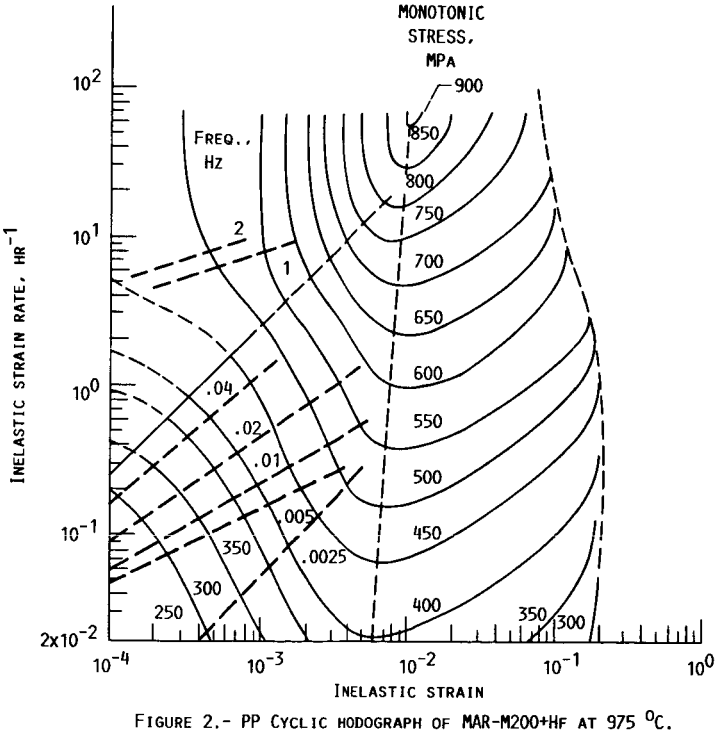

FIGURE 2.- PP CYCLIC HODOGRAPH OF MAR-M200+HF AT 975 ^{o}C.

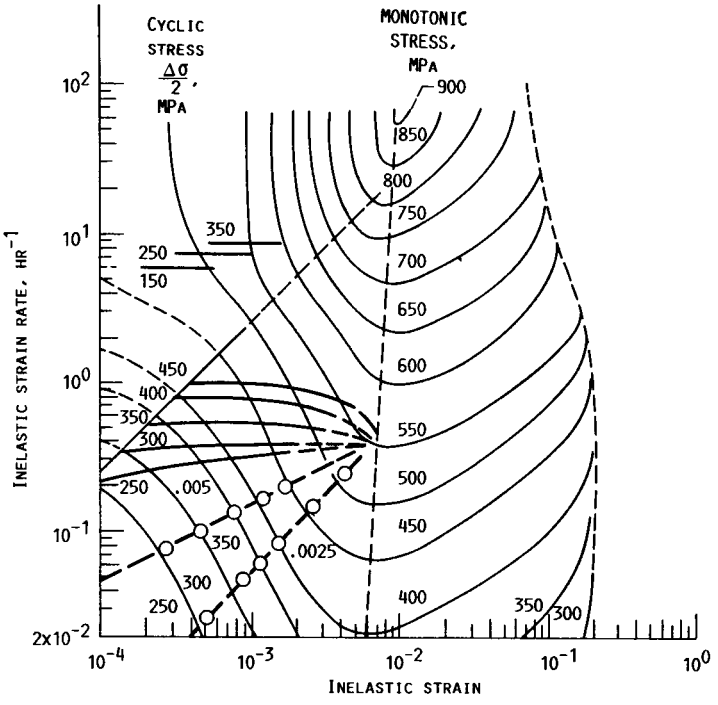

FIGURE 3.- CC CYCLIC HODOGRAPH FOR MAR-M200+HF AT 975 °C.

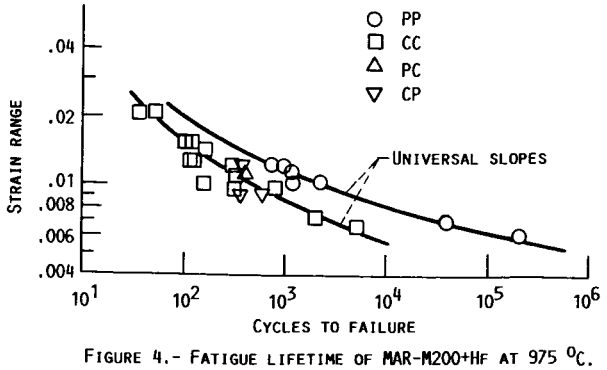

FIGURE 4.- FATIGUE LIFETIME OF MAR-M200+HF AT 975 °C.

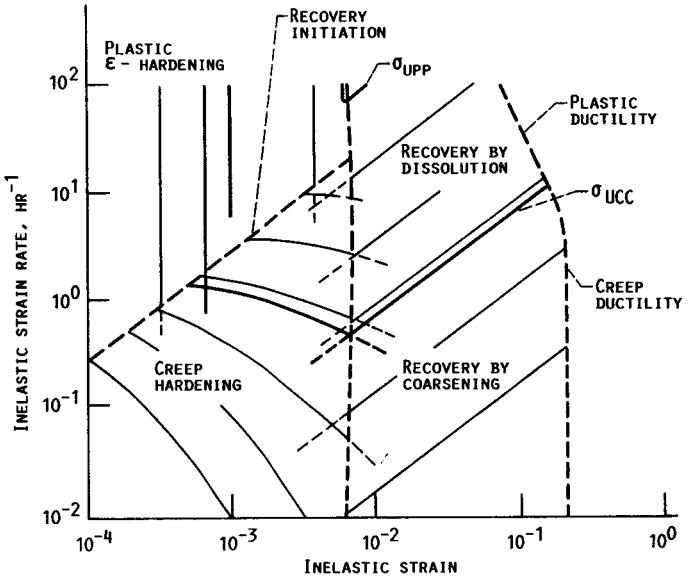

FIGURE 5.- COMPONENTS OF CONSTITUTIVE MODEL.

1. Report No.	2. Government Accession No.	3. Recipient's Catalog No.
NASA TM-88841		

4. Title and Subtitle	5. Report Date
Estimation of High Temperature Low Cycle Fatigue on the Basis of Inelastic Strain and Strainrate	6. Performing Organization Code: 505-63-11

7. Author(s)	8. Performing Organization Report No.
A. Berkovits	E-3168
	10. Work Unit No.

9. Performing Organization Name and Address	11. Contract or Grant No.
National Aeronautics and Space Administration Lewis Research Center Cleveland, Ohio 44135	13. Type of Report and Period Covered: Technical Memorandum

12. Sponsoring Agency Name and Address	14. Sponsoring Agency Code
National Aeronautics and Space Administration Washington, D.C. 20546	

15. Supplementary Notes

A. Berkovits, Summer Faculty Fellow.

16. Abstract

Fatigue life at elevated temperature can be predicted by introducing parametric values obtained from monotonic constitutive behavior into the Universal-Slopes Equation. For directionally solidified MAR-M200+Hf at 975 °C, these parameters are the maximum stress achievable under entirely plastic (time-independent) and purely creep (time-dependent) conditions and the corresponding inelastic strains, as well as the elastic modulus. For materials which exhibit plasticity/creep interaction, two more pairs of monotonic parameters must be evaluated for fatigue life prediction. This life-prediction method based on the Universal-Slopes Equation, resulted from a constitutive model characterizing monotonic and cyclic data as inelastic strainrate as a function of inelastic strain. Characterizing monotonic data in this way, permitted distinction between different material responses such as strain-hardening, strain-softening, and dynamic recovery effects. Understanding and defining the region of influence of each of these effects facilitated formulation of the constitutive model in relation to the mechanical and microstructural processes occurring in the material under cyclic loading.

17. Key Words (Suggested by Author(s))	18. Distribution Statement
Fatigue; High temperature; Low cycle; Inelastic strainrate; Superalloy; Creep; Plasticity; Strainrate	Unclassified - unlimited STAR Category 26

19. Security Classif. (of this report)	20. Security Classif. (of this page)	21. No. of pages	22. Price*
Unclassified	Unclassified		

*For sale by the National Technical Information Service, Springfield, Virginia 22161